Since January 2020 Elsevier has created a COVID-19 resource centre with free information in English and Mandarin on the novel coronavirus COVID-19. The COVID-19 resource centre is hosted on Elsevier Connect, the company's public news and information website.

Journal of Hazardous Materials 403 (2021) 123841

Contents lists available at ScienceDirect

Journal of Hazardous Materials

journal homepage: www.elsevier.com/locate/jhazmat

Gelatin/β–Cyclodextrin Bio–Nanofibers as respiratory filter media for filtration of aerosols and volatile organic compounds at low air resistance

Vinod Kadam [a,b,d,*], Yen Bach Truong [b], Jurg Schutz [c], Ilias Louis Kyratzis [b], Rajiv Padhye [a], Lijing Wang [a]

[a] School of Fashion & Textiles, RMIT University, Brunswick, Victoria 3056, Australia
[b] Commonwealth Scientific and Industrial Research Organization (CSIRO) - Manufacturing, Clayton, Victoria 3168, Australia
[c] Commonwealth Scientific and Industrial Research Organization (CSIRO) - Manufacturing, Waurn Ponds, VIC 3216, Australia
[d] ICAR–Central Sheep and Wool Research Institute, Rajasthan 304501, India

ARTICLE INFO

Editor: Xiaohong Guan

Keywords:
Air filtration
Particulate matter
Volatile organic compounds
Adsorption
Gelatin/β–cyclodextrin
Composite nanofibers
Respiratory protection
Pressure drop

ABSTRACT

Air pollution is a universal concern. The suspended solid/liquid particles in the air and volatile organic compounds (VOCs) are ubiquitous. Synthetic polymer-based air filter media not only has disposal issues but also is a source of air and water pollution at the end of their life cycle. It has been a challenge to filter both particulate matter and VOC pollutants by a common biodegradable filter media having low air resistance. This study reports gelatin/β–cyclodextrin composite nanofiber mats with dual function air filtration ability at reduced air resistance (148 Pa) and low basis weight (1 g/m^2). Gelatin/β–cyclodextrin nanofibers captured aerosols (0.3–5 μm) with < 95% filtration efficiency at 0.029/Pa quality factor. They adsorbed great amount of xylene (287 mg/g), benzene (242 mg/g), and formaldehyde (0.75 mg/g) VOCs. VOC adsorption of gelatin/β–cyclodextrin nanofibers is found several times higher than a commercial face mask and pristine powder samples. This study provides a solution for a 'green' dual function respiratory air filtration at low resistance. Gelatin/β–cyclodextrin nanofibers also have the potential to filter nano-sized viruses.

1. Introduction

The ubiquitous presence of air pollutants is taxing human health and hampering eco-system all over the globe (Lelieveld et al., 2015; Kampa and Castanas, 2008). Airborne solid/liquid droplets or aerosols, also known as particulate matter (PM), can cause respiratory and cardiovascular diseases leading to cancer and death (Qiu et al., 2015; Dai et al., 2015). The severity of the hazard mainly depends on the aerodynamic diameter of the PM. The particles having aerodynamic diameter ≤ 2.5 μm are defined as PM2.5 while PM10 indicates aerosols of size 2.5–10 μm (Kadam et al., 2018a). Smaller size particles cause higher risk to human health since they can be easily inhaled and penetrate the lungs without any resistance.

Volatile organic compounds (VOCs) represent another type of air pollutants, perhaps more harmful than the visible aerosols (Kadam, 2018; Bernstein et al., 2004). They can be carcinogenic, toxic and hazardous (Hong et al., 2017; Tsai, 2016, 2019). Formaldehyde, for instance, is one of the carcinogenic VOCs commonly found indoors and very hazardous even at lower concentrations. NIOSH recommended indoor exposure limit of formaldehyde is 0.019 mg/m^3 for 15 min (Anon., 2017) while its alarming threshold in US, China and Australia (>0.1 mg/m^3) (Rovira et al., 2016; Brown, 2002). Formaldehyde exposures can mainly cause pulmonary function damage and reproduction impairment (Kim et al., 2011; Han et al., 2015). Benzene and xylene are commonly used industrial chemicals and their prolonged exposure is hazardous. NIOSH recommended threshold limiting value is 31 mg/m^3 and 434 mg/m^3 for benzene and xylene, respectively (Kadam, 2018). Immediately dangerous to life or health (IDLH) values for formaldehyde, benzene and xylene are 20 ppm, 500 ppm and 900 ppm, respectively (Zhang et al., 2017). It is believed that the human body will be more susceptible to air pollutants due to unknown bio-physiochemical interactions with the increasing complexity of air pollutants, rapid industrialization and more urbanized lifestyle. Therefore, a dual-function air filter is a critical need for human health.

Multifunctional air filter refers to simultaneous filtration of solid/liquid droplets of various size as well as gaseous VOCs. However, designing multifunctional filters has been challenging since the filtration mechanism of PM and VOCs is entirely different. PM and VOCs vary in

* Corresponding author at: School of Fashion & Textiles, RMIT University, Brunswick, Victoria 3056, Australia.
E-mail address: vinod.vjti@gmail.com (V. Kadam).

https://doi.org/10.1016/j.jhazmat.2020.123841
Received 27 May 2020; Received in revised form 2 August 2020; Accepted 27 August 2020
Available online 3 September 2020

size and chemical composition (Kadam et al., 2018a; Bernstein et al., 2004). PM filtration depends on fiber diameter and pore size. The diffusion, interception, straining, electrostatic attraction and gravitational forces are the principles of PM capture (Kadam et al., 2018a; Kadam, 2018; Mukhopadhyay, 2010). VOC filtration depends on physical and chemical adsorption which requires functional polymer surface (Kadam et al., 2018a).

Air filtration is the first commercially successful application of electrospun nanofibers (Kadam et al., 2018a; Kadam, 2018). Electrospinning is an application of high electrical voltage to a polymer fluid to produce 1D nanosized fibers (Kadam et al., 2018a; Zhu et al., 2017; Xue et al., 2019). It has been a widely accepted technique for producing polymeric nanofibers due to its tuneable fiber morphology, versatility (Xue et al., 2019), high specific surface area, compactness and excellent mechanical properties (Al-Attabi et al., 2018). The synthetic polymers such as polyacrylonitrile, polyamide, polysulfone have been electrospun for air filtration due to their excellent strength and environment stability (Kadam et al., 2018a; Al-Attabi et al., 2018; Wang et al., 2015). However, to use them as an advanced dual-function air filter, there are limitations like poor surface functionality of synthetic polymers necessary for VOC adsorption. Besides, synthetic polymer degradability after disposal is a serious environmental concern (Moore, 2008; Miller, 2013; Souzandeh et al., 2019). Synthetic polymers continue to release harmful VOCs even after disposal (Lomonaco et al., 2020) and recycling (Cabanes et al., 2020). Synthetic polymers also have lethal effects on aquatic and terrestrial ecosystem (Singh et al., 2020). Hence, biodegradable and functional polymers can be the better choice for multifunctional air filters.

Gelatin is a low cost and abundantly available protein biopolymer obtained from partial hydrolysis of collagen found in various biomaterials (Liu et al., 2019). It has been widely explored in biomedical applications such as tissue engineering, drug delivery and wound healing (Ko et al., 2010; Erencia et al., 2015; Rath et al., 2016). Recently, gelatin nanofiber was studied for air filtration where environmental susceptibility of gelatin has been addressed by carbodiimide cross-linking (Zhang et al., 2010; Campiglio et al., 2019). The cross-linked gelatin nanofibers showed environmental stability, better mechanical properties and comparable filtration performance (Deng et al., 2019). Gelatin nanofibers also showed anti-bacterial efficacy (Souzandeh et al., 2017). Gelatin can absorb gas pollutants due to its surface functionality. However, VOC adsorption performance of gelatin electrospun nanofibers is not known.

β–Cyclodextrin (β–CD) is a commercially available, low priced cyclic oligosaccharide (Del Valle, 2004; Taka et al., 2017). It is a non-hygroscopic, torus-shaped crystalline substance isolated from starch digestion (Szejtli, 1998; Medronho et al., 2013). β–CD has seven repeating glucose units linked via α-1,4-glucosidic bonds in a cone-shaped structure (Zhao et al., 2015; Wu et al., 2015; Celebioglu and Uyar, 2012; Marques, 2010). It is a non-toxic and biodegradable material (Morin-Crini et al., 2018). β–CD has been studied for water filtration (Alsbaiee et al., 2016), air filtration (Kadam et al., 2018b; Wang et al., 2019a) and drug delivery applications (Aytac et al., 2019; Wang et al., 2019b) due to its reactive nature and a typical cone-shaped cavity structure. Our previous work (Kadam et al., 2018b) did show that β–CD and polyacrylonitrile nanofibers improved VOC adsorption. β–CD combination with gelatin can offer further reactivity (Liu et al., 2013; Lee et al., 2016; Chen et al., 2018) along with resolving sustainability and biodegradability issues.

In this paper, gelatin/β–cyclodextrin composite nanofiber mats were prepared using electrospinning for multifunctional air filtration. The effect of various concentrations of β–CD on composite nanofibers was studied using SEM, capillary flow porometry, surface area analyser and FTIR. Air filtration was evaluated for KCl aerosols of size 0.3–5 μm. VOC adsorption was studied for three models VOCs namely formaldehyde, xylene and benzene. The adsorption performance was compared with a commercial face mask.

2. Experimental

2.1. Materials

Gelatin (from porcine skin, Type A) and β-cyclodextrin powder were obtained from Sigma Aldrich, Australia. The solvents, formic acid (98–100%) and ethanol (99.5%) were obtained from Merck, Australia. Xylene (Merck, Australia), benzene (Merck, Australia) and formaldehyde (37% formalin, Chem-supply, Australia) solutions were used to generate respective VOC vapours under controlled conditions (Temperature 20 ± 3 °C; humidity 50 ± 2%). All the chemicals were employed as received without any further purification. The control nonwoven fabric (polyester viscose (50:50)) was kindly supplied by Textor Ltd. Australia. The control fabric had a basis weight of 45 g/m^2, thickness 0.16 mm and pore size 12 μm. Commercial P2 type masks were purchased from the local market in Melbourne, Australia.

2.2. Methods

Gelatin powder (16% w/w) was dissolved in the formic acid at room temperature. β–CD powder was added in different proportions (10%, 20% and 30% w/w) to the gelatin solution and stirred until a homogenous solution was obtained. The terminology used to describe the various solutions was G, GC1, GC2 and GC3. G represented only gelatin while GC1, GC2 and GC3 represented the addition of 10%, 20% and 30% β–CD over the weight of gelatin, respectively. Before electrospinning, the composite solution was centrifuged using a rotor (JA 25.50) at 9000 rpm for 15 min to remove any undissolved particles. The viscosity of solutions was measured using a viscometer (Brookfield DV-II + Pro) with a spindle number of SC4−21.

The solution was electrospun using a laboratory electrospinning setup (Kadam, 2018; Kadam et al., 2018b, 2019). In brief, the installation consists of a rack-mounted DC voltage supply (Spellman SL150), a syringe pump (NE1000 New Era Pump Systems, Inc.) and a metal surfaced drum collector. The electrospinning parameters employed were: 22 kV applied voltage, 0.15 mL/h flow rate and 20 cm distance from the needle (23 gauge) tip to drum surface. The nanofibers were deposited on the collector covered with the control nonwoven fabric. The surface density of gelatin nanoweb (1 g/m^2) was obtained using Eq. (1).

$$m = \frac{c_p\ \rho_s\ r_f\ t_s}{a_c} \quad (1)$$

Where, m is basis weight of nanoweb, c_p is polymer concentration, ρ_s is the solution density, r_f is feed rate, t_s is electrospinning time and a_c is collector area (19cm × 34 cm). After electrospinning, nanofibers were dried overnight at room temperature followed by drying in a vacuum oven for 4 h at 50 °C. The electrospinning experiments were conducted at room temperature (23 ± 2 °C) and relative humidity of 50 ± 2%.

2.3. Nanofiber mat characterization

Nanofibers were sputter-coated with iridium for morphology analysis. The morphology of nanofibers was studied using a field emission scanning electron microscope (FE-SEM) (Zeiss, Gemini 2 Merlin) at 3 kV acceleration voltage. From FE-SEM images, the fiber diameter was measured using ImageJ software. The pore size of nanofibers was measured using the capillary flow porometer (Porous Materials Inc) by measuring the pressure gradient (Eq. (2)) needed to displace Galwick liquid (Surface tension 15.9 mN m^{-1}) through pore capillaries of nanofiber structure. The average of three nanofiber samples of 13 mm diameter was used to measure pore size and its distribution over the pressure range of 0–30 PSI.

$$dp = \frac{4\sigma cos\theta}{\Delta p} \quad (2)$$

where σ is the surface tension of the wetting liquid (N/m), θ is the contact angle that the wetting liquid forms with the filter and ΔP is the differential pressure (Pa) applied across the filter.

The specific surface area of nanofiber samples was determined using BET surface area analyser (Nova 1200e, Quantachrome Instruments). The values were determined from their adsorption and desorption isotherms of nitrogen at −196 °C using a Quantachrome Autosorb-1 volumetric adsorption system. The samples were degassed under vacuum at 40 °C for 22 h before analysis. The nanofiber membranes were also characterised using Fourier transform infrared (FTIR) spectroscopy (Thermo Nicolet 6700) in the range of 4000–800 cm^{-1}. Total 64 number of scans were performed for each sample to generate FTIR spectra. Energy dispersive X-ray (EDX) spectroscopy was done by analysing SEM images with the help of Xmax80 detector and Aztec software platform for determination of elemental composition. Five different areas were averaged for the elemental analysis.

2.4. Air filtration and VOC adsorption measurement

The air filtration of nanofiber mats was measured using the experimental set up reported elsewhere (Kadam, 2018; Kadam et al., 2018b). In short, the aerosols of average sizes of 0.3–5 μm were generated in the atomiser using 20 wt% KCl solution. The aerosols of known concentration flow through the rig at a flow rate of 20 L/min (face velocity 0.06 m/s) and eventually hit the nanofiber mat filter media. The difference in particle concentration and pressure before and after filtration was measured to describe filtration efficiency (Eq. (3)) and pressure drop (Eq. (4)), respectively. The filtration efficiency and pressure drop are opposite to each other. The term quality factor (Eq. (5)) combines filtration efficiency and pressure drop to express an overall filtration performance indicator.

$$\eta = \frac{n_1 - n_2}{n_1} \tag{3}$$

$$\Delta P = P_1 - P_2 \tag{4}$$

$$Q = \frac{-\ln\left(\frac{n_2}{n_1}\right)}{\Delta p} = \frac{-\ln\left(1-\eta\right)}{\Delta p} \tag{5}$$

where: n_1: Upstream aerosol particle concentration (number); n_2: Downstream aerosol particle concentration (number); P_1: Upstream absolute air pressure (Pa); P_2: Downstream absolute air pressure (Pa).

VOC adsorption performance was measured using a simple laboratory setup reported elsewhere in detail (Kadam, 2018; Kadam et al., 2018b, 2020). Briefly, a known quantity of xylene or benzene analyte was injected into a plastic jar (4.5 L) with a specially designed lid. The lid had rubber septa at the top, steel wire with a hook, and a mesh to hold the sample. The analyte was exposed to the sample for 4 h in the airtight jar kept in the conditioned room (20 ± 2 °C and 50 ± 3% RH). The sample was then immersed in 15 mL ethanol for 24 h to extract the VOC (xylene or benzene) analyte completely. The concentration of xylene and benzene was determined using UV–vis spectroscopy at the characteristic absorbance of 268 nm and 255 nm, respectively. Standard calibration curves were obtained for different concentrations of xylene and benzene (Kadam, 2018; Kadam et al., 2018b, 2020). Three readings of VOC adsorption were averaged. For HCHO, UV spectroscopy did not show any unique peak. The residual HCHO was determined using a formaldemeter™ (PPM Technology) and subtracted from the plain reading (empty jar without any sample) to evaluate adsorption performance.

Table 1
Viscosity of the gelatin and gelatin blended solutions of different amounts of β–CD.

Sample	Details	Viscosity (cP) at room temperature	Electrical conductivity (μS/cm)
G	16% (w/w) gelatin	502.4	650
GC1	16% (w/w) gelatin +10 wt% β–CD	518.4	844
GC2	16% (w/w) gelatin +20 wt% β–CD	566.0	698
GC3	16% (w/w) gelatin +30 wt% β–CD	637.6	549

3. Results and discussion

3.1. Solution properties

Table 1 shows the viscosity of the pure gelatin solution (16% w/w) and the solutions prepared from gelatin mixing with different concentrations of β–CD. The gelatin solution shows the viscosity of 502.4 cP (mPa.s). For reproducible gelatin nanofibers, the solution viscosity is constrained in the range of 200–1500 cP (Erencia et al., 2015). The addition of 10% β–CD slightly increased the viscosity of gelatin solution from 502.4 cP to 518.4 cP. Further addition of β–CD (20% and 30%) increased the viscosity to 566 cP and 637.6 cP, respectively. The high viscosity of the solutions resists the free movement of molecules hence the flow rate during the electrospinning was on the lower side.

Unlike viscosity, the conductivity results in Table 1 did not show a linear trend. The highest conductivity recorded for GC1 (844 μS/cm). The increase in conductivity can be due to the presence of hydroxyl group of β–CD in GC1 solution with that of G. However, further increasing the concentration β–CD as in case of GC2 and GC3, the conductivity decreased (698 μS/cm and 549 μS/cm, respectively). This trend is in line with our previous study (Kadam et al., 2018b) where the reduction of conductivity was noticed at higher concentrations of β–CD. The reduction is due to the restricted ionic mobility caused by the high viscosity of the solution containing a high amount of β–CD.

3.2. Gelatin-β–CD nanomembrane characterization

Electrospinning of gelatin (16% w/w) (G) resulted in the average fiber diameter of 130 nm (Fig. 1a). FE-SEM images in Fig. 1b–d show an increasing sequence of gelatin nanofiber diameters (130–247 nm) upon the addition of β–CD (GC1–GC3). This change in mean fiber diameter was attributed to the rise in the solution viscosity (502–637 cP) which is due to the increasing concentration of β-CD. Solution viscosity affects the spinnability, the morphology of the electrospun nanofibers as well as the fiber diameter (Ramakrishna et al., 2005; Butcher et al., 2017). Although the viscosity was found to dominate over conductivity, the decreased conductivity contributes to the increase of the fiber diameter. Low conductivity reduces the bending instability in the jet which causes an increase in the fiber diameter (Bhardwaj and Kundu, 2010). The nanofiber diameter appears in normal frequency distribution (Fig. 1) in all the combinations from G to GC3. It indicates homogeneity of gelatin solutions after addition of β–CD in different proportions consequently resulting in symmetry around the mean fiber diameters in each case.

Besides fluid characteristics, optimizing the electrospinning parameters has a paramount impact on defect-free composite nanofibers production and homogenous fiber distribution (Al-Attabi et al., 2019). Herein, the optimized parameters (as mentioned in methods) resulted in uniform composite nanofibers of gelatin/β–CD and no phase separation was observed upon storage for several weeks after electrospinning, despite low areal density (1 g/m^2). Nanofibers are difficult to maintain structural integrity due to their delicacy (Sundarrajan et al., 2014). Nonwoven porous support preserved the structural integrity of gelatin/β–CD nanofibers during handling, storage, characterisation, and filtration performance measurement.

Another interesting observation in FE-SEM images of electrospun gelatin is the frequent occurrence of “web” structures (Fig. 2). Web in this context may be referred to densely superimposed and interconnected fibers which are much smaller dimension than nanofibers.

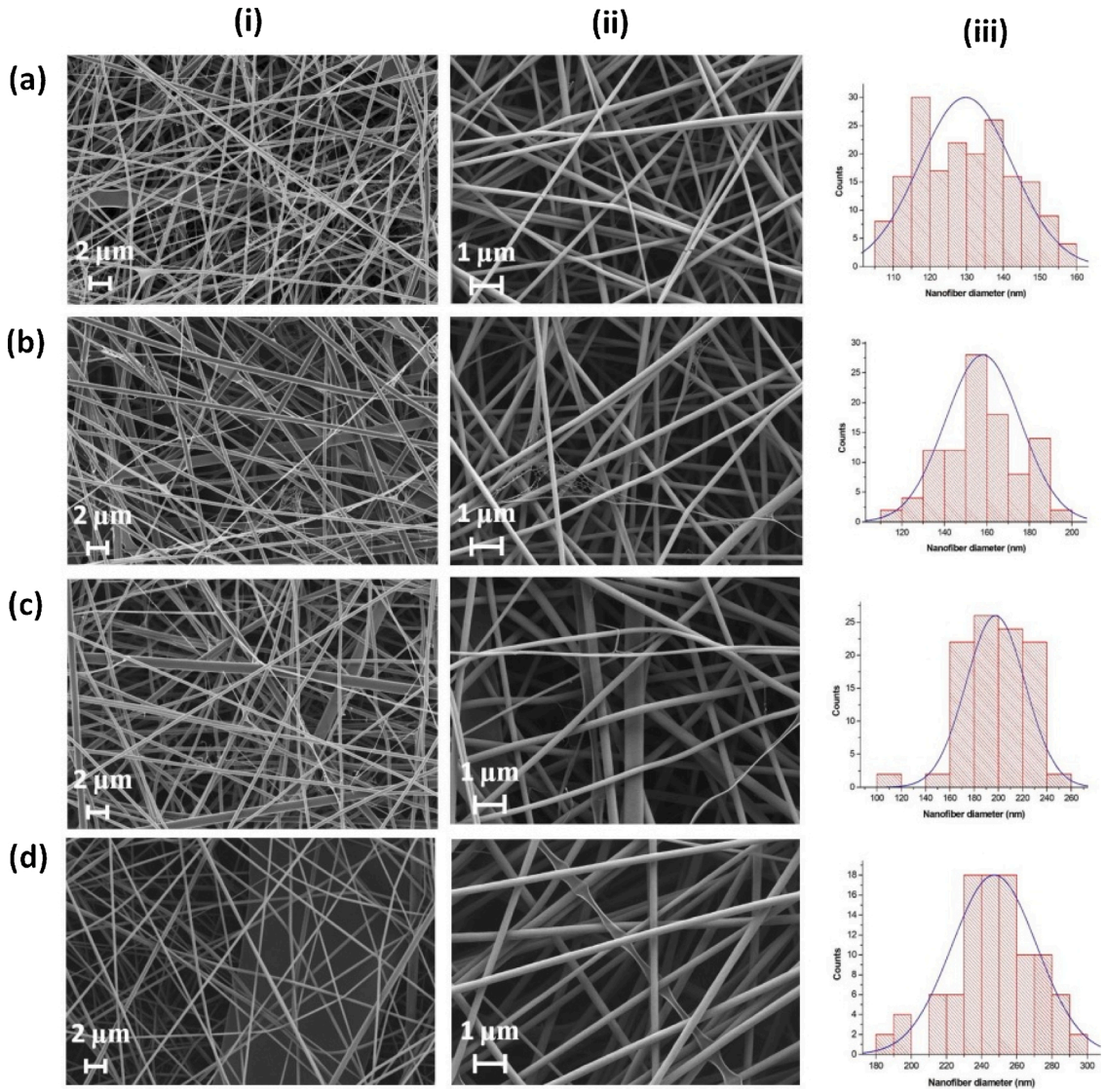

Fig. 1. FE-SEM images of gelatin-β–CD composite nanofibers (a) G (130 ± 13 nm); (b) GC1 (158 ± 18 nm); (c) GC2 (198 ± 24 nm); (d) GC3 (247 ± 24 nm) at (i) X5000, (ii) X10,000 (iii) nanofiber diameter distribution.

The interconnected tiny fibers in the webs were not used for fiber diameter measurement. These webs look like cobwebs but the web fiber diameter is much smaller (< 50 nm) as compared to the nanofiber diameter. Such webs could be useful for air filtration to capture PM2.5 as well as tiny sized viruses including coronavirus (Leung and Sun, 2020). It is (Maze et al., 2007) simulated that nanofibers made of 50–200 nm showed the most penetrating particle size of 100–200 nm. Thus, the gelatin nanofiber mat is a potential candidate in the preparation of biomaterial based nanofiber mats for air filtration and respiratory protection. However, the frequency of the webs disappeared in GC2 and GC3 which is probably due to the increase in solution viscosity after incorporation of higher amounts of β–CD.

Table 2 shows the EDX elemental analysis of gelatin/β–CD composite nanofibers. It can be seen that gelatine nanofiber is composed of 69% carbon (C), 21.7% nitrogen (N) and 8.9% oxygen (O). The addition of β–CD greatly reduced nitrogen and increased oxygen. The N/C ratio was highly reduced from 0.31 to 0.12 during the conversion of G into GC1. However, the N/C ratio is found comparable for GC1 to GC3, unlike the O/C ratio, which is increased with the β–CD concentration due to the oxygen-rich structure of β–CD (Kadam et al., 2020).

Pore size is an important parameter for air filtration applications. Through pores of small size are desirable for maximum filtration efficiency (Kadam et al., 2018a). Table 3 describes the pore size dimensions of gelatin/β–CD nanofiber mat. The pore size is in the range of 0.97–1.43 µm despite the fiber diameter is much smaller (130–247 nm). This is because small areal density of the nanofiber meshes (1 g/m^2) created more inter-fiber spaces. The average pore size increases as the β-CD concentration increases. An increase in gelatin nanofiber diameter subsequently leads to an increase in the pore size (Joy et al., 2018).

Pore size distribution can influence filtration efficiency and pressure drop (Krifa and Yuan, 2016). The pore size was found to be normally distributed and the center shifted towards right from G to GC3 (Fig. 3). This shift indicates an increase in pore size which is the result of an increase in fiber diameter from G to GC3. The specific surface area depends on fiber diameter. The smaller fiber diameter of G (130 nm) showed the highest surface area (124.7 m^2/g) (Table 3). GC3 (247 nm mean fiber diameter) resulted in the lowest specific surface area (37.3 m^2/g) because the increase in fiber diameter greatly reduces the specific surface area. This reduction can influence the air filtration performance which is discussed in the later section.

Fig. 4 presents FTIR spectra of gelatin powder, CD powder, gelatin and composite gelatin β–CD nanofiber mats. The gelatin powder (Fig. 4a) displays characteristic peaks at 3290 cm^{-1}, 1646 cm^{-1} 1537 cm^{-1} and 1233 cm^{-1}, corresponding to a hydroxyl group (−OH), Amide

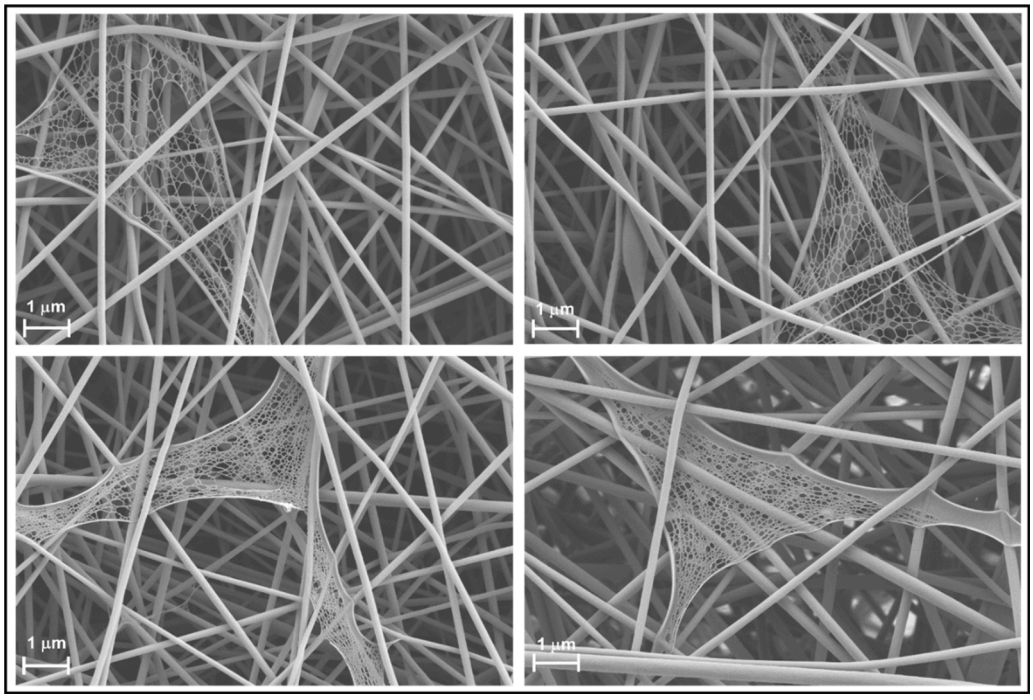

Fig. 2. Webs embedded in gelatin 16% (w/w) nanofiber mat.

Table 2
EDX elemental analysis of gelatin β–CD composite nanofibers.

Nanofiber	C %	N %	O %	N/C	O/C
G	69.0	21.7	8.9	0.31	0.13
GC1	78.0	9.8	11.0	0.12	0.14
GC2	77.4	8.7	12.9	0.11	0.16
GC3	73.6	9.6	15.7	0.13	0.21

Table 3
Pore size determined using capillary flow porometer and surface area of nanofiber mat determined using BET surface area analyser.

Nanofiber mat	Pore size (μm)			Surface area (m^2/g)
	Smallest	Average	Highest (Bubble point)	
G	0.80	0.97	1.60	124.70
GC1	0.89	1.00	1.30	111.03
GC2	0.87	1.19	1.54	92.07
GC3	1.04	1.43	1.75	37.32

A, Amide I, Amide II and Amide III, respectively (Irfanita et al., 2017; Derkach et al., 2019). Amide A refers to gelatin specific N—H stretching (Sengor et al., 2020). Amide-I is associated with C=O stretching, Amide II is due to C—N stretch and Amide III is related to in-plane N—H deformation (Biswal et al., 2019). Also, small peaks at 1446 cm^{-1}, 1337 cm^{-1} and 1085 cm^{-1} were due to symmetric and asymmetric $-CH_3$ bending vibrations (Das et al., 2017) and –C-C stretching, respectively (Calixto et al., 2019). The characteristic peaks for β–CD (Fig. 4b) at 1023 cm^{-1}, 1077 cm^{-1} and 1179 cm^{-1} correspond to C—O stretching of the acetal group in the glucopyranoside units of the β–CD (Kadam et al., 2018b). The peak at 3286 cm^{-1} indicates intermolecular bonded O—H stretching within the β–CD. Most of these peak frequencies also remain unchanged during the addition process (Fig. 4c). However, the peak 1023 cm^{-1} shifted to 1054 cm^{-1}, indicating possible interaction of β–CD with gelatin (Fig. 4d). The additional peak at 1077 cm^{-1} and 1179 cm^{-1} appeared in GC1, GC2 and GC3 which confirms the presence of β–CD

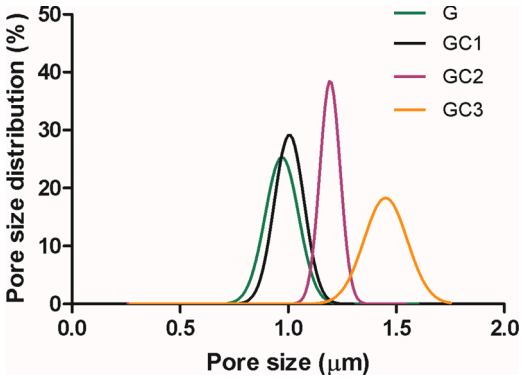

Fig. 3. The pore size distribution of G, GC1, GC2 and GC3 nanofiber mats obtained at a differential pressure range of 0–30 PSI using Galwick fluid (Surface tension 15.9 dynes/cm) in capillary flow porometer.

functional groups on the composite gelatin/β–CD nanofiber mat.

3.3. Air filtration performance

Fig. 5 shows the air filtration performance of gelatin/β–CD nanofiber mats for particle sizes ranging from 0.3 μm to 5 μm at 0.06 m/s face velocity. The filtration efficiency of G, GC1 and GC2 was found to be comparable for 0.3 μm and 5 μm particles (around 97% and 99%, respectively). While GC3 reduced the filtration efficiency (88%) due to the coarse fiber diameter (247 nm) and low surface area (37 m^2/g) as compared to that of G (nanofiber diameter 130 nm; surface area 124 m^2/g). The results infer that β–CD addition up to 20% produces comparable air filtration performance to that of only gelatin nanofibers. The efficiency (97%) of gelatin/β–CD for 0.3 μm particles is slightly lower than the recent report (98%) (Souzandeh et al., 2017) possibly due to the smaller basis weight (1 g/m^2) and higher average fiber diameter (130 nm) compared to the reported one (2 g/m^2 and 87 nm, respectively). However, the efficiency of gelatin/β–CD nanofibers (97%) is better than a P2 type mask (94%). For particles ≥ 0.7 μm the efficiency is beyond

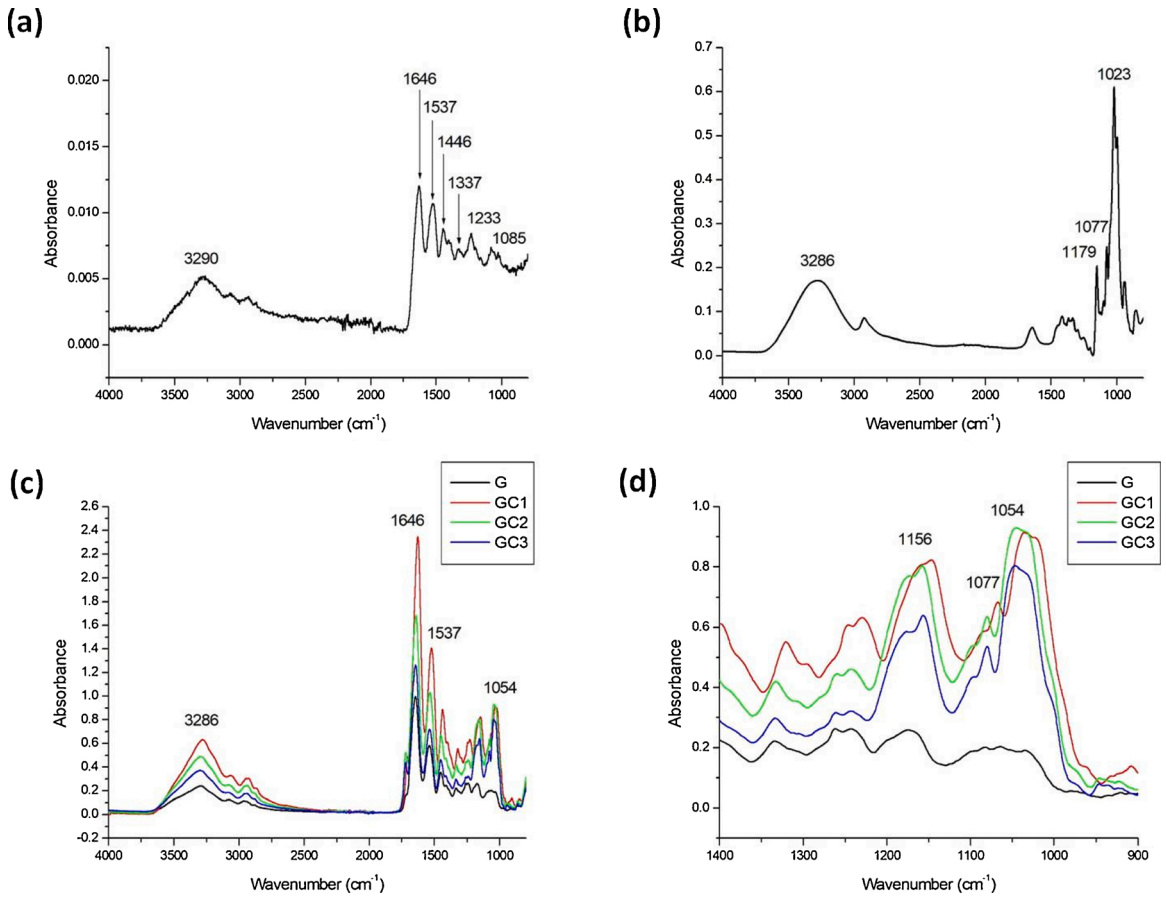

Fig. 4. FTIR spectra of (a) gelatin powder, (b) β–CD powder, (c) normalized gelatin β–CD composite nanofiber mats over the range of 4000–800 cm^{-1} and (d) magnified spectra of composite nanofibers over the range of 1400–900 cm^{-1}.

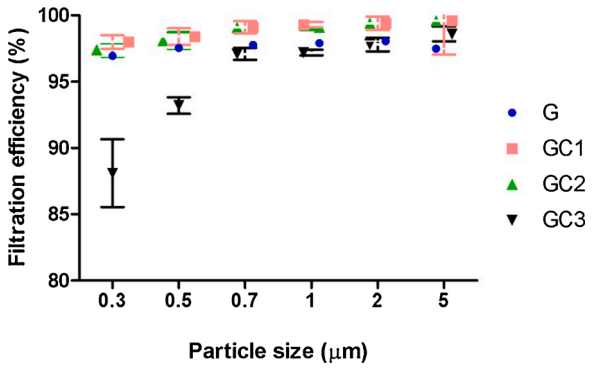

Fig. 5. Filtration efficiency of gelatin/β–CD nanofiber mats (1 g/m^2) at 0.06 m/s face velocity.

99%. The high filtration efficiency is due to the effective diffusion and interception mechanism of nanofibers (Kadam et al., 2019, 2017).

Fig. 6a shows the pressure drop of the gelatin and gelatin/β–CD nanofiber mats of 1 g/m^2 at 0.06 m/s face velocity. The gelatin nanofiber mat exhibited the highest pressure drop (163 Pa), due to the smallest fiber diameter (130 nm). The pressure drop of GC1 and GC2 nanofiber mats is comparable (151 Pa VS 148 Pa) since the fiber diameter of both nanofiber mats ranged between 160–200 nm. GC3 nanofiber mat having the largest average fiber diameter (247 nm) shows the lowest pressure drop (125 Pa) which is comparable to P2 type mask (120 Pa). The low-pressure drop ensures low air resistance and high breathability. The pressure drop of GC1 and GC2 was found lower than that of gelatin electrospun mats (180 Pa) reported recently (Souzandeh et al., 2017). However, a direct comparison between pressure drops of nanofibers is not appropriate since pressure drop is affected by many parameters like material dimensions (basis weight, thickness, pore size distribution and fiber diameter distribution) and test parameters (flow rate, face velocity and filter sample size). Gelatin nanofibers in this study are better in terms of low pressure drop and high filtration efficiency at 1 g/m^2 basis weight and 0.06 m/s face velocity.

The quality factor is an overall representation of air filtration performance where the outcome of filtration efficiency and pressure drop combined (Kadam et al., 2018a). It is noteworthy that the quality factor of gelatin-based nanofiber mats is being reported for the first time. It can be seen in Fig. 6b that the quality factor of gelatin nanofiber mats improved (from 0.021/Pa to 0.029/Pa) due to the addition of β–CD. The reduction in pressure drop (from 163 Pa to 148 Pa) at comparable filtration efficiency (97%) caused this improvement. Further addition of β–CD (30%), however, deteriorated the quality factor (0.017/Pa) despite a reduction in pressure drop (125 Pa). This deterioration of quality factor is attributed to the loss in filtration efficiency (88%) compared to other nanofiber mats (97%). The basis weight of the nanofiber mat can strongly influence the quality factor (Kadam et al., 2019). It this work, the maximum quality factor of 0.029/Pa was achieved for GC2 at 1 g/m^2, which is better than 0.024/Pa as reported earlier (Liu et al., 2015) and at par (0.028/Pa) as reported recently (Kadam et al., 2018b) on polyacrylonitrile nanofiber mats at a similar basis weight of 1 g/m^2.

A commercial N95 type mask has the filtration efficiency of >95% (Rengasamy et al., 2017) and pressure drop of 11 mm (108 Pa) (Janssen, 2004). However, the basis weight of N95 masks is more than 500 g/m^2

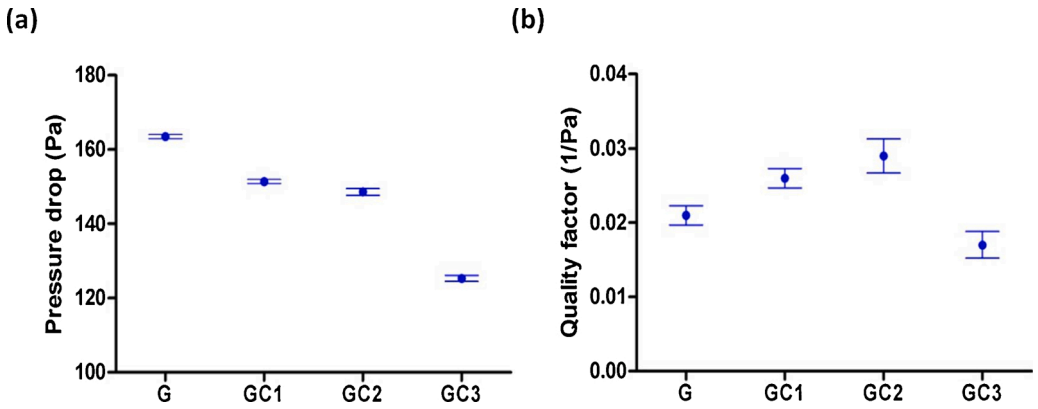

Fig. 6. (a) Pressure drop and (b) quality factor of gelatin/β–CD composite nanofiber mats for 0.3 μm particles at 0.06 m/s face velocity.

which induces thermal stress to wearer (Roberge et al., 2012; Li et al., 2005). Herein, gelatin/β–CD nanofiber media achieved >95% filtration efficiency at 1 g/m^2 basis weight. The filtration efficiency is comparable to that of the conventional facemask. Moreover, this mat is environmentally friendly and comfortable regarding the weight lightness.

3.4. VOC adsorption

Activated carbon is preferably used in filter media for VOC adsorption due to its high surface area (higher than nanofibers) and porous structure (Pei and Zhang, 2011). However, it is not effective for solid/liquid aerosols; it has poor chemical functionality and short service life (Kadam, 2018). Activated carbon has practical limitations concerning handling and reusability (Celebioglu et al., 2016). Since the particles of activated carbon are easily inhalable, proper care, maintenance and training are required while using respirators enabled with activated carbon. No such drawbacks are associated with nanofibers.

The xylene adsorption by a commercial facemask and individual powder samples of gelatin and β–CD was studied for comparison. The powder sample was wrapped in the porous nonwoven fabric which was used to deposit nanofiber mats during electrospinning. As shown in Fig. 7a, xylene adsorption of gelatin powder (23 mg/g) is marginally higher than β–CD powder (14 mg/g). Whereas, P2 type face mask shows least xylene adsorption (2 mg/g).

Gelatin nanofiber mat showed the highest xylene adsorption (311 mg/g) which is 150 times of the commercial face mask (2 mg/g) and 13 times of gelatin powder form (23 mg/g) (Fig. 7a). With increasing levels of β–CD addition GC1 to GC3, xylene adsorption reduced (287–250 mg/g). The results can be linked with the increase in fiber diameter from 130 nm to 247 nm, as the xylene VOC adsorption is influenced by the fiber diameter. The xylene adsorption of gelatin was found much higher than our result on PAN/β–CD composite nanofiber mat (201 mg/g) (Kadam et al., 2018b) and β–CD cross-linked fabric (11 mg/g) (Kadam et al., 2020). It is mainly due to gelatin and a multi-fold increase in the specific surface area of gelatin nanofiber mat. This performance was found much better than adsorbing only 0.04 mg/g xylene by polyurethane/fly ash composite nanofibers reported (Kim et al., 2013).

Benzene adsorption (Fig. 7b) is found in line with xylene adsorption since they have a similar chemical structure. Gelatin nanofiber mat showed the highest benzene adsorption (279 mg/g) which again can be explained by the smallest fiber diameter (130 nm) and highest surface area. The benzene adsorption of GC1 and GC2 was found comparable (around 242 mg/g) since their fiber diameter range is also comparable. GC3 displayed the lowest benzene adsorption (176 mg/g) explained by the larger fiber diameter (247 nm). The adsorption performance of β–CD powder (12.49 mg/g) was slightly higher than the gelatin powder (11.58 mg/g) due to cavities in the structure β–CD. P2 type mask has least benzene adsorption (5.27 mg/g).

Although β–CD can form complex with aromatic xylene and benzene, no significant increase in xylene and benzene adsorption by the composite gelatin/β–CD nanofibers mats (GC1, GC2 and GC3) was observed. The adsorption was found more dependent on fiber diameter and specific surface area than the use of β–CD in electrospinning. The adsorption of xylene and benzene VOCs was not found material-specific/adsorbent specific, unlike formaldehyde which may be due to the relative inertness of xylene and benzene. Hence, any nanoscale materials having a high surface area would physically adsorb these VOCs.

Fig. 7c shows HCHO adsorption performance. It can be seen that the commercial mask has negligible HCHO adsorption (0.002 mg/g) while the nonwoven fabric without nanofibers showed only little (0.02 mg/g) adsorption (Kadam et al., 2020). β–CD powder has relatively higher HCHO adsorption (0.07 mg/g) than the gelatin powder (0.04 mg/g). When gelatin was converted into nanofibers the adsorption increased by ten times (0.38 mg/g). This rise is attributed to the smallest diameter (130 nm), higher surface area (124 m^2/g) and protein structure of electrospun gelatin fiber. HCHO, being reactive electrophilic species, reacts with functional groups of gelatin by cross-linking with N-terminal amino acid residue and the side chains of arginine, cysteine, histidine and lysine residues (Metz et al., 2004). The cross-linking is induced by primary amines (lysine) forming a stable methylene bridge (Thavarajah et al., 2012).

The composite gelatin/β–CD mats (GC1–GC3) further improved the HCHO adsorption (0.75 mg/g), unlike xylene and benzene VOCs. Although GC1, GC2 and GC3 showed comparable HCHO adsorption, there is a clear advantage of using β–CD for better HCHO adsorption than the gelatin only. The increase in HCHO adsorption can be due to host-guest complex formation and weak physical interactions induced by β–CD.

The HCHO adsorption by composite gelatin/β–CD nanofibers mats (0.75 mg/g) is better that by polyacrylonitrile/β–CD nanofibers (0.07 mg/g) (Kadam et al., 2018b) and β–CD cross-linked textiles (0.06 mg/g) (Kadam et al., 2020). The HCHO adsorption value from this work (0.75 mg/g) is also higher than the 0.12 mg/mg of PAN/β–CD nanofibers (Noreña-Caro and Álvarez-Láinez, 2016). However, it is much less than that of activated carbon fiber (roughly 24 mg/g) (Rong et al., 2003). Recently, around 70% HCHO removal efficiency was reported using PVA/soy protein nanofibers (Souzandeh et al., 2016) and gelatin nanofibers (Souzandeh et al., 2017) of 4.5 g/m^2 basis weight. Although a direct comparison cannot be made, relative advantage of lightness can help in designing better multifunctional respiratory filter media.

4. Conclusion

Gelatin/β–CD composite solutions have been successfully electrospun to produce nanofiber mats with a fiber diameter ranging 130–247 nm. It is found that β–CD addition (10% and 20%) in gelatin

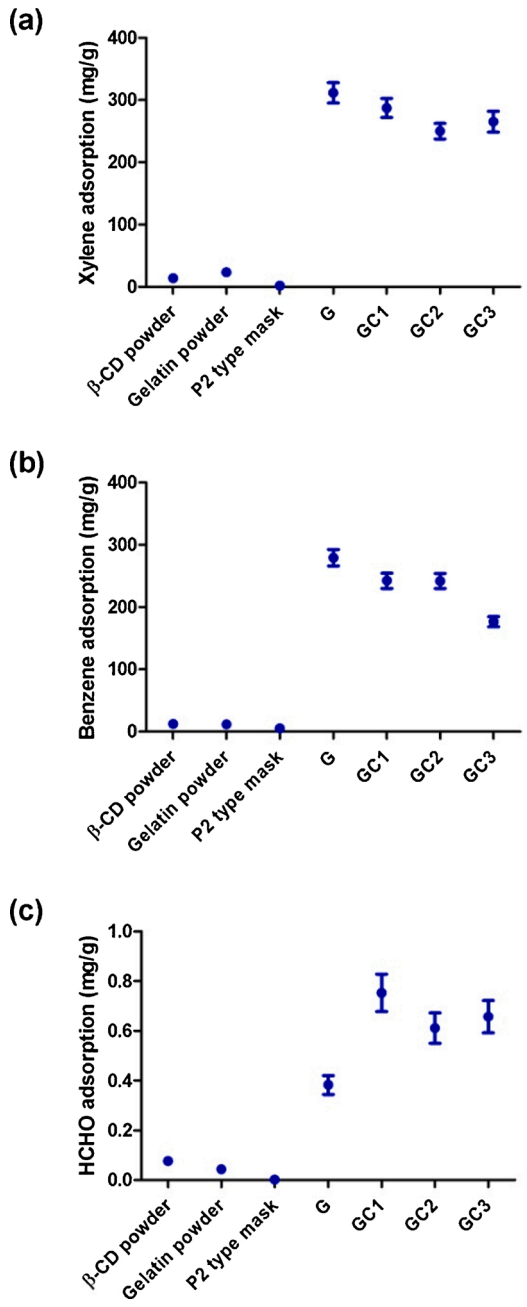

Fig. 7. VOCs adsorption performance of gelatin and β–CD powder, P2 mask and gelatin/β–CD nanofiber mats. (a) Xylene adsorption, the values were obtained using UV spectroscopy at the characteristic wavelength of 268 nm. (b) Benzene adsorption, the adsorbed benzene was extracted using ethanol and analysed by UV spectroscopy at the characteristic wavelength of 255 nm (c) HCHO adsorption performance using formalhydemeter.

electrospinning yielded comparable filtration efficiency (97% for 0.3 μm and $<$ 99% for particles $\geq$ 0.7 μm), lower pressure drop (148 Pa) and improved quality factor (0.029/Pa) at 1 g/m^2 basis weight. Gelatin/β–CD composite nanofibers showed excellent adsorption of xylene (287 mg/g), benzene (242 mg/g) and formaldehyde (0.75 mg/g). β–CD is found most beneficial in formaldehyde adsorption while xylene and benzene adsorption is observed to be influenced by the fiber diameter and the specific surface area of nanofibers. The gelatin/β–CD biomaterial-based nanofibers filtered solid/liquid aerosols and gaseous pollutants simultaneously at lower basis weight with low air resistance. The combination of gelatin/β–CD nanofibers with their green nature, excellent dual function filtration, less air resistance and potential to capture tiny viruses make them suitable for respiratory filtration.

CRediT authorship contribution statement

Vinod Kadam: Conceptualization, Investigation, Writing - original draft. **Yen Bach Truong:** Data curation, Resources, Software, Supervision. **Jurg Schutz:** Data curation, Formal analysis. **Ilias Louis Kyratzis:** Methodology, Validation. **Rajiv Padhye:** Funding acquisition, Project administration. **Lijing Wang:** Writing - review & editing, Supervision.

Declaration of Competing Interest

No conflict of interest to declare.

Acknowledgements

Vinod Kadam would like to acknowledge Research Stipend Scholarship of Royal Melbourne Institute of Technology (RMIT) University, Australia for financial support, and the Indian Council of Agricultural Research (ICAR), India for granting his study leave.

References

Al-Attabi, R., Morsi, Y., Schütz, J., Dumée, L., 2018. Electrospun membranes for airborne contaminants capture. Handbook of Nanofibers, pp. 1–18.
Al-Attabi, R., Rodriguez-Andres, J., Schütz, J.A., Bechelany, M., Des Ligneris, E., Chen, X., Kong, L., Morsi, Y.S., Dumée, L.F., 2019. Catalytic electrospun nanocomposite membranes for virus capture and remediation. Sep. Purif. Technol. 229, 115806.
Al-Attabi, R., Dumée, L.F., Kong, L., Schütz, J.A., Morsi, Y., 2018. High efficiency poly (acrylonitrile) electrospun nanofiber membranes for airborne nanomaterials filtration. Adv. Eng. Mater. 20, 1700572.
Alsbaiee, A., Smith, B.J., Xiao, L., Ling, Y., Helbling, D.E., Dichtel, W.R., 2016. Rapid removal of organic micropollutants from water by a porous β-cyclodextrin polymer. Nature 529, 190–194.
Anon, 2017. In: Labor, U.S.Do. (Ed.), Occupational, Safety, A. Health, Formaldehyde. United States Department of Labor USA.
Aytac, Z., Ipek, S., Erol, I., Durgun, E., Uyar, T., 2019. Fast-dissolving electrospun gelatin nanofibers encapsulating ciprofloxacin/cyclodextrin inclusion complex. Colloids Surf. B 178, 129–136.
Bernstein, J.A., Alexis, N., Barnes, C., Bernstein, I.L., Nel, A., Peden, D., Diaz-Sanchez, D., Tarlo, S.M., Williams, P.B., Bernstein, J.A., 2004. Health effects of air pollution. J. Allergy Clin. Immunol. 114, 1116–1123.
Bhardwaj, N., Kundu, S.C., 2010. Electrospinning: a fascinating fiber fabrication technique. Biotechnol. Adv. 28, 325–347.
Biswal, A.K., Samal, A.K., Tripathy, M., Misra, P.K., 2019. Identification of the secondary structure of protein isolated from deoiled cake flour of Mahua (Madhuca latifolia). Mater. Today Proc. 9, 605–614.
Brown, S.K., 2002. Volatile organic pollutants in new and established buildings in Melbourne, Australia. Indoor Air 12, 55–63.
Butcher, A.L., Koh, C.T., Oyen, M.L., 2017. Systematic mechanical evaluation of electrospun gelatin meshes. J. Mech. Behav. Biomed. Mater. 69, 412–419.
Cabanes, A., Valdés, F., Fullana, A., 2020. A review on VOCs from recycled plastics. Sustain. Mater. Technol. e00179.
Calixto, S., Piazza, V., Marañon-Ruiz, V.F., 2019. Stimuli-responsive systems in optical humidity-detection devices. Materials 12, 327.
Campiglio, C.E., Contessi Negrini, N., Farè, S., Draghi, L., 2019. Cross-linking strategies for electrospun gelatin scaffolds. Materials 12, 2476.
Celebioglu, A., Uyar, T., 2012. Electrospinning of nanofibers from non-polymeric systems: polymer-free nanofibers from cyclodextrin derivatives. Nanoscale 4, 621–631.
Celebioglu, A., Sen, H.S., Durgun, E., Uyar, T., 2016. Molecular entrapment of volatile organic compounds (VOCs) by electrospun cyclodextrin nanofibers. Chemosphere 144, 736–744.
Chen, Y., Ma, Y., Lu, W., Guo, Y., Zhu, Y., Lu, H., Song, Y., 2018. Environmentally friendly gelatin/β-cyclodextrin composite fiber adsorbents for the efficient removal of dyes from wastewater. Molecules 23, 2473.
Dai, J., Chen, R., Meng, X., Yang, C., Zhao, Z., Kan, H., 2015. Ambient air pollution, temperature and out-of-hospital coronary deaths in Shanghai, China. Environ. Pollut. 203, 116–121.
Das, M.P., Suguna, P., Prasad, K., Vijaylakshmi, J., Renuka, M., 2017. Extraction and characterization of gelatin: a functional biopolymer. Int. J. Pharm. Pharm. Sci. 9, 239–242.
Del Valle, E.M.M., 2004. Cyclodextrins and their uses: a review. Process. Biochem. 39, 1033–1046.
Deng, L., Li, Y., Feng, F., Zhang, H., 2019. Study on wettability, mechanical property and biocompatibility of electrospun gelatin/zein nanofibers cross-linked by glucose. Food Hydrocoll. 87, 1–10.

Derkach, S.R., Voron'ko, N.G., Sokolan, N.I., Kolotova, D.S., Kuchina, Y.A., 2019. Interactions between gelatin and sodium alginate: UV and FTIR studies. J. Dispersion Sci. Technol. 1–9.
Erencia, M., Cano, F., Tornero, J.A., Fernandes, M.M., Tzanov, T., Macanás, J., Carrillo, F., 2015. Electrospinning of gelatin fibers using solutions with low acetic acid concentration: effect of solvent composition on both diameter of electrospun fibers and cytotoxicity. J. Appl. Polym. Sci. 132.
Han, S.-P., Zhou, D.-X., Lin, P., Qin, Z., An, L., Zheng, L.-R., Lei, L., 2015. Formaldehyde exposure induces autophagy in testicular tissues of adult male rats. Environ. Toxicol. 30, 323–331.
Hong, S.-H., Shin, D.-C., Lee, Y.-J., Kim, S.-H., Lim, Y.-W., 2017. Health risk assessment of volatile organic compounds in urban areas. Hum. Ecol. Risk Assess. 23, 1454–1465.
Irfanita, N., Jaswir, I., Mirghani, M., Sukmasari, S., Ardini, Y., Lestari, W., 2017. Rapid detection of gelatin in dental materials using attenuated total reflection fourier transform infrared spectroscopy (ATR-FTIR). In: Journal of Physics: Conference Series. IOP Publishing, p. 012090.
Janssen, L.L., 2004. Efficiency and pressure drop effects of high concentrations of cement dust on N95 electret filters. J. Int. Soc. Respir. Prot. 21.
Joy, J., Pereira, J., Aid-Launais, R., Pavon-Djavid, G., Ray, A.R., Letourneur, D., Meddahi-Pellé, A., Gupta, B., 2018. Gelatin—oxidized carboxymethyl cellulose blend based tubular electrospun scaffold for vascular tissue engineering. Int. J. Biol. Macromol. 107, 1922–1935.
Kadam, V., 2018. Multifunctional air filtration for respiratory protection using electrospun nanofibre membrane, in: School of Fashion and Textiles. RMIT University, Melbourne, p. 182.
Kadam, V., Truong, Y., Kyratzis, I., Wang, L., Padhye, R., 2017. Bilayer electrospun nanofibre structures to improve quality factor in air filtration. NewTech'17: The 3rd World Congress on New Technologies. Avestia Publishing, pp. 1–9.
Kadam, V.V., Wang, L., Padhye, R., 2018a. Electrospun nanofibre materials to filter air pollutants – a review. J. Ind. Text. 47, 2253–2280.
Kadam, V., Truong, Y.B., Easton, C., Mukherjee, S., Wang, L., Padhye, R., Kyratzis, I.L., 2018b. Electrospun polyacrylonitrile/β-Cyclodextrin composite membranes for simultaneous air filtration and adsorption of volatile organic compounds. Acs Appl. Nano Mater. 1, 4268–4277.
Kadam, V., Kyratzis, I.L., Truong, Y.B., Schutz, J., Wang, L., Padhye, R., 2019. Electrospun bilayer nanomembrane with hierarchical placement of bead-on-string and fibers for low resistance respiratory air filtration. Sep. Purif. Technol. 224, 247–254.
Kadam, V., Kyratzis, I.L., Truong, Y.B., Wang, L., Padhye, R., 2020. Air filter media functionalized with β-Cyclodextrin for efficient adsorption of volatile organic compounds. J. Appl. Polym. Sci. 137, 49228.
Kampa, M., Castanas, E., 2008. Human health effects of air pollution. Environ. Pollut. 151, 362–367.
Kim, K.-H., Jahan, S.A., Lee, J.-T., 2011. Exposure to formaldehyde and its potential human health hazards. J. Environ. Sci. Health Part C 29, 277–299.
Kim, H.J., Pant, H.R., Choi, N.J., Kim, C.S., 2013. Composite electrospun fly ash/polyurethane fibers for absorption of volatile organic compounds from air. Chem. Eng. J. 230, 244–250.
Ko, J.H., Yin, H.Y., An, J., Chung, D.J., Kim, J.-H., Lee, S.B., Pyun, D.G., 2010. Characterization of cross-linked gelatin nanofibers through electrospinning. Macromol. Res. 18, 137–143.
Krifa, M., Yuan, W., 2016. Morphology and pore size distribution of electrospun and centrifugal forcespun nylon 6 nanofiber membranes. Text. Res. J. 86, 1294–1306.
Lee, J.B., Kim, J.E., Balikov, D.A., Bae, M.S., Heo, D.N., Lee, D., Rim, H.J., Lee, D.W., Sung, H.J., Kwon, I.K., 2016. Poly (l-lactic acid)/gelatin fibrous scaffold loaded with simvastatin/beta-cyclodextrin-modified hydroxyapatite inclusion complex for bone tissue regeneration. Macromol. Biosci. 16, 1027–1038.
Lelieveld, J., Evans, J., Fnais, M., Giannadaki, D., Pozzer, A., 2015. The contribution of outdoor air pollution sources to premature mortality on a global scale. Nature 525, 367–371.
Leung, W.W.-F., Sun, Q., 2020. Charged PVDF multilayer nanofiber filter in filtering simulated airborne novel coronavirus (COVID-19) using ambient nano-aerosols. Sep. Purif. Technol. 245, 116887.
Li, Y., Tokura, H., Guo, Y., Wong, A., Wong, T., Chung, J., Newton, E., 2005. Effects of wearing N95 and surgical facemasks on heart rate, thermal stress and subjective sensations. Int. Arch. Occup. Environ. Health 78, 501–509.
Liu, C., Zhang, Z., Liu, X., Ni, X., Li, J., 2013. Gelatin-based hydrogels with β-cyclodextrin as a dual functional component for enhanced drug loading and controlled release. RSC Adv. 3, 25041–25049.
Liu, C., Hsu, P.C., Lee, H.W., Ye, M., Zheng, G., Liu, N., Li, W., Cui, Y., 2015. Transparent air filter for high-efficiency PM2. 5 capture. Nat. Commun. 6, 6205.
Liu, Y., Ng, S.C., Yu, J., Tsai, W.-B., 2019. Modification and crosslinking of gelatin-based biomaterials as tissue adhesives. Colloids Surf. B 174, 316–323.
Lomonaco, T., Manco, E., Corti, A., La Nasa, J., Ghimenti, S., Biagini, D., Di Francesco, F., Modugno, F., Ceccarini, A., Fuoco, R., 2020. Release of harmful volatile organic compounds (VOCs) from photo-degraded plastic debris: a neglected source of environmental pollution. J. Hazard. Mater. 122596.
Marques, H.M.C., 2010. A review on cyclodextrin encapsulation of essential oils and volatiles. Flav. Fragrance J. 25, 313–326.
Maze, B., Vahedi, T.H., Wang, Q., Pourdeyhimi, B., 2007. A simulation of unsteady-state filtration via nanofiber media at reduced operating pressures. J. Aerosol Sci. 38, 550–571.
Medronho, B., Andrade, R., Vivod, V., Ostlund, A., Miguel, M.G., Lindman, B., Voncina, B., Valente, A.J., 2013. Cyclodextrin-grafted cellulose: physico-chemical characterization. Carbohydr. Polym. 93, 324–330.
Metz, B., Kersten, G.F., Hoogerhout, P., Brugghe, H.F., Timmermans, H.A., De Jong, A., Meiring, H., ten Hove, J., Hennink, W.E., Crommelin, D.J., 2004. Identification of formaldehyde-induced modifications in proteins reactions with model peptides. J. Biol. Chem. 279, 6235–6243.
Miller, S.A., 2013. Sustainable polymers: opportunities for the next decade. In: ACS Macro Letters, 2. ACS, pp. 550–554.
Moore, C.J., 2008. Synthetic polymers in the marine environment: a rapidly increasing, long-term threat. Environ. Res. 108, 131–139.
Morin-Crini, N., Winterton, P., Fourmentin, S., Wilson, L.D., Fenyvesi, E., Crini, G., 2018. Water-insoluble β-cyclodextrin–epichlorohydrin polymers for removal of pollutants from aqueous solutions by sorption processes using batch studies: a review of inclusion mechanisms. Prog. Polym. Sci. 78, 1–23.
Mukhopadhyay, A., 2010. Pulse-jet filtration: an effective way to control industrial pollution Part II: process characterization and evaluation of filter media. Text. Prog. 42, 1–97.
Noreña-Caro, D., Álvarez-Láinez, M., 2016. Functionalization of polyacrylonitrile nanofibers with β-cyclodextrin for the capture of formaldehyde. Mater. Des. 95, 632–640.
Pei, J., Zhang, J.S., 2011. On the performance and mechanisms of formaldehyde removal by chemi-sorbents. Chem. Eng. J. 167, 59–66.
Qiu, H., Tian, L., Ho, K., Pun, V.C., Wang, X., Yu, I.T.S., 2015. Air pollution and mortality: effect modification by personal characteristics and specific cause of death in a case-only study. Environ. Pollut. 199, 192–197.
Ramakrishna, S., Fujihara, K., Teo, W.-E., Lim, T.-C., Ma, Z., 2005. An Introduction to Electrospinning and Nanofibers. World Scientific.
Rath, G., Hussain, T., Chauhan, G., Garg, T., Goyal, A.K., 2016. Development and characterization of cefazolin loaded zinc oxide nanoparticles composite gelatin nanofiber mats for postoperative surgical wounds. Mater. Sci. Eng. 58, 242–253.
Rengasamy, S., Shaffer, R., Williams, B., Smit, S., 2017. A comparison of facemask and respirator filtration test methods. J. Occup. Environ. Hyg. 14, 92–103.
Roberge, R., Benson, S., Kim, J.-H., 2012. Thermal burden of N95 filtering facepiece respirators. Ann. Occup. Hyg. 56, 808–814.
Rong, H., Ryu, Z., Zheng, J., Zhang, Y., 2003. Influence of heat treatment of rayon-based activated carbon fibers on the adsorption of formaldehyde. J. Colloid Interface Sci. 261, 207–212.
Rovira, J., Roig, N., Nadal, M., Schuhmacher, M., Domingo, J.L., 2016. Human health risks of formaldehyde indoor levels: an issue of concern. J. Environ. Sci. Health Part A 51, 357–363.
Sengor, M., Ozgun, A., Gunduz, O., Altintas, S., 2020. Aqueous electrospun core/shell nanofibers of PVA/microbial transglutaminase cross-linked gelatin composite scaffolds. Mater. Lett. 263, 127233.
Singh, R.P., Mishra, S., Das, A.P., 2020. Synthetic microfibers: pollution toxicity and remediation. Chemosphere 127199.
Souzandeh, H., Johnson, K.S., Wang, Y., Bhamidipaty, K., Zhong, W.-H., 2016. Soy-protein-based nanofabrics for highly efficient and multifunctional air filtration. ACS Appl. Mater. Interfaces 8, 20023–20031.
Souzandeh, H., Molki, B., Zheng, M., Beyenal, H., Scudiero, L., Wang, Y., Zhong, W.-H., 2017. Cross-linked protein nanofilter with antibacterial properties for multifunctional air filtration. ACS Appl. Mater. Interfaces 9, 22846–22855.
Souzandeh, H., Wang, Y., Netravali, A.N., Zhong, W.-H., 2019. Towards Sustainable and Multifunctional Air-Filters: A Review on Biopolymer-Based Filtration Materials. Polym. Rev. 59, 651–686.
Sundarrajan, S., Tan, K.L., Lim, S.H., Ramakrishna, S., 2014. Electrospun nanofibers for air filtration applications. Procedia Eng. 75, 159–163.
Szejtli, J., 1998. Introduction and general overview of cyclodextrin chemistry. Chem. Rev. 98, 1743–1754.
Taka, A.L., Pillay, K., Mbianda, X.Y., 2017. Nanosponge cyclodextrin polyurethanes and their modification with nanomaterials for the removal of pollutants from waste water: a review. Carbohydr. Polym. 159, 94–107.
Thavarajah, R., Mudimbaimannar, V.K., Elizabeth, J., Rao, U.K., Ranganathan, K., 2012. Chemical and physical basics of routine formaldehyde fixation. J. Oral Maxillofac. Pathol. 16, 400.
Tsai, W.-T., 2016. Toxic volatile organic compounds (VOCs) in the atmospheric environment: regulatory aspects and monitoring in Japan and Korea. Environments 3, 23.
Tsai, W.-T., 2019. An overview of health hazards of volatile organic compounds regulated as indoor air pollutants. Rev. Environ. Health 34, 81–89.
Wang, N., Yang, Y., Al-Deyab, S.S., El-Newehy, M., Yu, J., Ding, B., 2015. Ultra-light 3D nanofibre-nets binary structured nylon 6–polyacrylonitrile membranes for efficient filtration of fine particulate matter. J. Mater. Chem. A 3, 23946–23954.
Wang, L., Kang, Y., Xing, C.-Y., Guo, K., Zhang, X.-Q., Ding, L.-S., Zhang, S., Li, B.-J., 2019a. β-Cyclodextrin based air filter for high-efficiency filtration of pollution sources. J. Hazard. Mater. 373, 197–203.
Wang, J., Guo, Z., Xiong, J., Wu, D., Li, S., Tao, Y., Qin, Y., Kong, Y., 2019b. Facile synthesis of chitosan-grafted beta-cyclodextrin for stimuli-responsive drug delivery. Int. J. Biol. Macromol. 125, 941–947.
Wu, H., Kong, J., Yao, X., Zhao, C., Dong, Y., Lu, X., 2015. Polydopamine-assisted attachment of β-cyclodextrin on porous electrospun fibers for water purification under highly basic condition. Chem. Eng. J. 270, 101–109.
Xue, J., Wu, T., Dai, Y., Xia, Y., 2019. Electrospinning and electrospun nanofibers: methods, materials, and applications. Chem. Rev. 119, 5298–5415.
Zhang, X., Do, M.D., Casey, P., Sulistio, A., Qiao, G.G., Lundin, L., Lillford, P., Kosaraju, S., 2010. Chemical modification of gelatin by a natural phenolic cross-linker, tannic acid. J. Agric. Food Chem. 58, 6809–6815.

Zhang, X., Gao, B., Creamer, A.E., Cao, C., Li, Y., 2017. Adsorption of VOCs onto engineered carbon materials: a review. J. Hazard. Mater. 338, 102–123.
Zhao, R., Wang, Y., Li, X., Sun, B., Wang, C., 2015. Synthesis of β-cyclodextrin-based electrospun nanofiber membranes for highly efficient adsorption and separation of methylene blue. ACS Appl. Mater. Interfaces 7, 26649–26657.
Zhu, M., Han, J., Wang, F., Shao, W., Xiong, R., Zhang, Q., Pan, H., Yang, Y., Samal, S.K., Zhang, F., 2017. Electrospun nanofibers membranes for effective air filtration. Macromol. Mater. Eng. 302, 1600353.